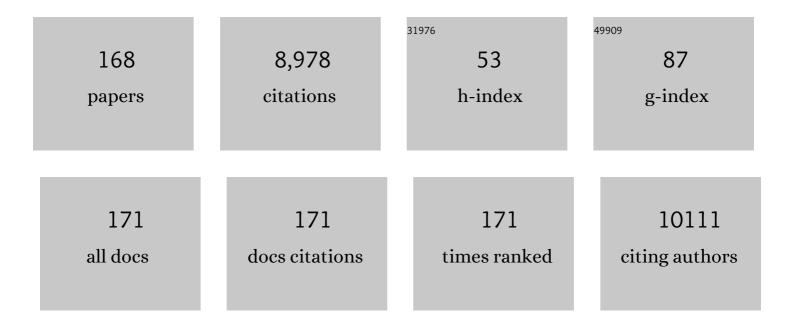
## Zidong Wang

List of Publications by Year in descending order

Source: https://exaly.com/author-pdf/72909/publications.pdf Version: 2024-02-01



#	Article	IF	CITATIONS
1	Labelâ€Free Colorimetric Detection of Lead Ions with a Nanomolar Detection Limit and Tunable Dynamic Range by using Gold Nanoparticles and DNAzyme. Advanced Materials, 2008, 20, 3263-3267.	21.0	426
2	Nanoparticle cluster gas sensor: Pt activated SnO <sub>2</sub> nanoparticles for NH <sub>3</sub> detection with ultrahigh sensitivity. Nanoscale, 2015, 7, 14872-14880.	5.6	284
3	Formaldehyde detection: SnO2 microspheres for formaldehyde gas sensor with high sensitivity, fast response/recovery and good selectivity. Sensors and Actuators B: Chemical, 2017, 238, 264-273.	7.8	280
4	DNA-Mediated Control of Metal Nanoparticle Shape: One-Pot Synthesis and Cellular Uptake of Highly Stable and Functional Gold Nanoflowers. Nano Letters, 2010, 10, 1886-1891.	9.1	278
5	Highly sensitive "turn-on―fluorescent sensor for Hg2+ in aqueous solution based on structure-switching DNA. Chemical Communications, 2008, , 6005.	4.1	253
6	Synthesis, characterization and photoluminescence of CeO2 nanoparticles by a facile method at room temperature. Journal of Alloys and Compounds, 2010, 493, 202-207.	5.5	224
7	A review on WO3 based gas sensors: Morphology control and enhanced sensing properties. Journal of Alloys and Compounds, 2020, 820, 153194.	5.5	200
8	Surfactant-assisted synthesis of CeO2 nanoparticles and their application in wastewater treatment. RSC Advances, 2012, 2, 12413.	3.6	186
9	Ordered Mesoporous Sb-, Nb-, and Ta-Doped SnO <sub>2</sub> Thin Films with Adjustable Doping Levels and High Electrical Conductivity. ACS Nano, 2009, 3, 1373-1378.	14.6	175
10	Antimony-Doped SnO <sub>2</sub> Nanopowders with High Crystallinity for Lithium-Ion Battery Electrode. Chemistry of Materials, 2009, 21, 3202-3209.	6.7	172
11	Novel Mixed Phase SnO <sub>2</sub> Nanorods Assembled with SnO <sub>2</sub> Nanocrystals for Enhancing Gas-Sensing Performance toward Isopropanol Gas. Journal of Physical Chemistry C, 2014, 118, 9832-9840.	3.1	146
12	A highly sensitive VOC gas sensor using p-type mesoporous Co3O4 nanosheets prepared by a facile chemical coprecipitation method. Sensors and Actuators B: Chemical, 2016, 233, 615-623.	7.8	137
13	A high response butanol gas sensor based on ZnO hollow spheres. Sensors and Actuators B: Chemical, 2016, 237, 423-430.	7.8	137
14	Functional DNA directed assembly of nanomaterials for biosensing. Journal of Materials Chemistry, 2009, 19, 1788.	6.7	129
15	Discovery of the DNA "Genetic Code―for Abiological Gold Nanoparticle Morphologies. Angewandte Chemie - International Edition, 2012, 51, 9078-9082.	13.8	128
16	Niobium Doped TiO <sub>2</sub> with Mesoporosity and Its Application for Lithium Insertion. Chemistry of Materials, 2010, 22, 6624-6631.	6.7	127
17	Acetone sensing performances based on nanoporous TiO2 synthesized by a facile hydrothermal method. Sensors and Actuators B: Chemical, 2017, 238, 491-500.	7.8	115
18	Nonaqueous synthesis of Ag-functionalized In2O3/ZnO nanocomposites for highly sensitive formaldehyde sensor. Sensors and Actuators B: Chemical, 2016, 224, 193-200.	7.8	114

#	Article	IF	CITATIONS
19	A facile hydrothermal synthesis of MnO <sub>2</sub> nanorod–reduced graphene oxide nanocomposites possessing excellent microwave absorption properties. RSC Advances, 2015, 5, 88979-88988.	3.6	113
20	Cd doped porous Co3O4 nanosheets as electrode material for high performance supercapacitor application. Electrochimica Acta, 2016, 196, 316-327.	5.2	113
21	DNAâ€Encoded Tuning of Geometric and Plasmonic Properties of Nanoparticles Growing from Gold Nanorod Seeds. Angewandte Chemie - International Edition, 2015, 54, 8114-8118.	13.8	109
22	Combustion synthesis of porous Pt-functionalized SnO <sub>2</sub> sheets for isopropanol gas detection with a significant enhancement in response. Journal of Materials Chemistry A, 2014, 2, 20089-20095.	10.3	106
23	Gas sensors based on TiO2 nanostructured materials for the detection of hazardous gases: A review. Nano Materials Science, 2021, 3, 390-403.	8.8	106
24	Highly sensitive formaldehyde gas sensor based on hierarchically porous Ag-loaded ZnO heterojunction nanocomposites. Sensors and Actuators B: Chemical, 2017, 247, 797-806.	7.8	100
25	A Highly Sensitive and Fast-Responding Ethanol Sensor Based on CdIn <sub>2</sub> O <sub>4</sub> Nanocrystals Synthesized by a Nonaqueous Solâ^'Gel Route. Chemistry of Materials, 2008, 20, 5781-5786.	6.7	93
26	Meso- and macroporous coral-like Co3O4 for VOCs gas sensor. Ceramics International, 2015, 41, 11004-11012.	4.8	93
27	A novel and sensitive ratiometric fluorescence assay for carbendazim based on N-doped carbon quantum dots and gold nanocluster nanohybrid. Journal of Hazardous Materials, 2020, 386, 121958.	12.4	92
28	A general nonaqueous sol-gel route to g-C3N4-coupling photocatalysts: the case of Z-scheme g-C3N4/TiO2 with enhanced photodegradation toward RhB under visible-light. Scientific Reports, 2016, 6, 39531.	3.3	85
29	Isopropanol sensing properties of coral-like ZnO–CdO composites by flash preparation via self-sustained decomposition of metal–organic complexes. Sensors and Actuators B: Chemical, 2014, 198, 402-410.	7.8	83
30	Electrochemical performance of W-doped anatase TiO2 nanoparticles as an electrode material for lithium-ion batteries. Journal of Materials Chemistry, 2011, 21, 6006.	6.7	81
31	Biomorphic synthesis of hollow CuO fibers for low-ppm-level n-propanol detection via a facile solution combustion method. Sensors and Actuators B: Chemical, 2016, 230, 1-8.	7.8	79
32	Hydrothermal Synthesis of <mml:math xmlns:mml="http://www.w3.org/1998/Math/MathML"&gt; <mml:mrow> <mml:msub> <mml:mrow> <mml:mtext>Sn( mathvariant="bold"&gt;2  </mml:mtext></mml:mrow></mml:msub> </mml:mrow> Nanostructures with Different Morphologies and Their Optical Properties. Journal of Nanomaterials, 2011, 2011, 1-10.</mml:math 	O2.7	text>
33	A two-dimensional Ti <sub>3</sub> C <sub>2</sub> T <sub><i>X</i></sub> MXene@TiO <sub>2</sub> /MoS <sub>2</sub> heterostructure with excellent selectivity for the room temperature detection of ammonia. Journal of Materials Chemistry A, 2022, 10, 5505-5519.	10.3	76
34	Enhanced formaldehyde sensing performance of 3D hierarchical porous structure Pt-functionalized NiO via a facile solution combustion synthesis. Sensors and Actuators B: Chemical, 2015, 220, 171-179.	7.8	75
35	Mesostructured SnO2 as sensing material for gas sensors. Solid-State Electronics, 2004, 48, 627-632.	1.4	74
36	A high-performance n-butanol gas sensor based on ZnO nanoparticles synthesized by a low-temperature solvothermal route. RSC Advances, 2015, 5, 54372-54378.	3.6	74

#	Article	IF	CITATIONS
37	Pd nanoparticles composited SnO2 microspheres as sensing materials for gas sensors with enhanced hydrogen response performances. Journal of Alloys and Compounds, 2017, 710, 216-224.	5.5	70

## Catalytic photodegradation of Congo red in aqueous solution by Ln(OH)3 (Ln = Nd, Sm, Eu, Gd, Tb, and) Tj ETQq0 $\begin{array}{c} 0 \\ 4.3 \\ 68 \end{array}$ rgBT /Overlock 10

39	Acetone detection properties of single crystalline tungsten oxide plates synthesized by hydrothermal method using cetyltrimethyl ammonium bromide supermolecular template. Sensors and Actuators B: Chemical, 2012, 162, 259-268.	7.8	66
40	Cerium oxide nanoparticles/multi-wall carbon nanotubes composites: Facile synthesis and electrochemical performances as supercapacitor electrode materials. Physica E: Low-Dimensional Systems and Nanostructures, 2017, 86, 284-291.	2.7	66
41	Ag–ZnO heterostructure nanoparticles with plasmon-enhanced catalytic degradation for Congo red under visible light. RSC Advances, 2015, 5, 34456-34465.	3.6	65
42	A high performance methanol gas sensor based on palladium-platinum-In2O3 composited nanocrystalline SnO2. Sensors and Actuators B: Chemical, 2016, 237, 133-141.	7.8	65
43	Electrochemical performance of mesoporous ZnCo2O4 nanosheets as an electrode material for supercapacitor. Ionics, 2018, 24, 2435-2443.	2.4	65
44	The high efficient catalytic properties for thermal decomposition of ammonium perchlorate using mesoporous ZnCo2O4 rods synthesized by oxalate co-precipitation method. Scientific Reports, 2018, 8, 7571.	3.3	63
45	Preparation and gas-sensing properties of NiFe2O4 semiconductor materials. Solid-State Electronics, 2005, 49, 1029-1033.	1.4	62
46	Surfactant CATB-assisted generation and gas-sensing characteristics of LnFeO3 (Ln=La, Sm, Eu) materials. Sensors and Actuators B: Chemical, 2009, 143, 124-131.	7.8	62
47	Facile synthesis of α-MnO2 nanorods at low temperature and their microwave absorption properties. Materials Chemistry and Physics, 2014, 143, 1061-1068.	4.0	62
48	Photocatalytic degradation properties of Ni(OH)2 nanosheets/ZnO nanorods composites for azo dyes under visible-light irradiation. Ceramics International, 2014, 40, 57-65.	4.8	62
49	Electrochemical performance of CeO2 nanoparticle-decorated graphene oxide as an electrode material for supercapacitor. Ionics, 2017, 23, 121-129.	2.4	62
50	A simple method to prepare Ln(OH)3 (Ln=La, Sm, Tb, Eu, and Gd) nanorods using CTAB micelle solution and their room temperature photoluminescence properties. Journal of Alloys and Compounds, 2011, 509, 2060-2065.	5.5	59
51	Shaddock peels as bio-templates synthesis of Cd-doped SnO2 nanofibers: A high performance formaldehyde sensing material. Journal of Alloys and Compounds, 2020, 813, 152170.	5.5	59
52	Lanthanum Dioxide Carbonate La2O2CO3 Nanorods as a Sensing Material for Chemoresistive CO2 Gas Sensor. Electrochimica Acta, 2014, 127, 355-361.	5.2	57
53	SnO2 nanostructured materials used as gas sensors for the detection of hazardous and flammable gases: A review. Nano Materials Science, 2022, 4, 339-350.	8.8	57
54	Preparation and characterization of MnOOH and β-MnO 2 whiskers. Inorganic Chemistry Communication, 2002, 5, 747-750.	3.9	56

#	Article	IF	CITATIONS
55	SnO2 nanorods based sensing material as an isopropanol vapor sensor. New Journal of Chemistry, 2014, 38, 2443.	2.8	56
56	Microwave absorption characteristics of manganese dioxide with different crystalline phase and nanostructures. Materials Chemistry and Physics, 2010, 124, 639-645.	4.0	53
57	The xylene sensing performance of WO <sub>3</sub> decorated anatase TiO <sub>2</sub> nanoparticles as a sensing material for a gas sensor at a low operating temperature. RSC Advances, 2016, 6, 49692-49701.	3.6	53
58	Construction of novel Pd–SnO2 composite nanoporous structure as a high-response sensor for methane gas. Journal of Alloys and Compounds, 2020, 826, 154063.	5.5	53
59	Structural and photocatalytic properties of nickel-doped zinc oxide powders with variable dopant contents. Journal of Physics and Chemistry of Solids, 2013, 74, 1196-1203.	4.0	52
60	Porous NiO nanosheets self-grown on alumina tube using a novel flash synthesis and their gas sensing properties. RSC Advances, 2015, 5, 4880-4885.	3.6	52
61	Enhanced microwave absorption properties of MnO2 hollow microspheres consisted of MnO2 nanoribbons synthesized by a facile hydrothermal method. Journal of Alloys and Compounds, 2016, 676, 224-230.	5.5	52
62	Effects of calcining temperature on the phase structure and the formaldehyde gas sensing properties of CdO-mixed In2O3. Sensors and Actuators B: Chemical, 2008, 135, 219-223.	7.8	51
63	Jute-based porous biomass carbon composited by Fe3O4 nanoparticles as an excellent microwave absorber. Journal of Alloys and Compounds, 2019, 803, 1119-1126.	5.5	51
64	Controllable synthesis and change of emission color from green to orange of ZnO quantum dots using different solvents. New Journal of Chemistry, 2015, 39, 2881-2888.	2.8	50
65	Raspberry-like SnO 2 hollow nanostructure as a high response sensing material of gas sensor toward n-butanol gas. Journal of Physics and Chemistry of Solids, 2018, 120, 173-182.	4.0	50
66	Gas sensing materials roadmap. Journal of Physics Condensed Matter, 2021, 33, 303001.	1.8	49
67	Morphology control of porous CuO by surfactant using combustion method. Applied Surface Science, 2015, 349, 844-848.	6.1	47
68	Gas-sensing performances of Cd-doped ZnO nanoparticles synthesized by a surfactant-mediated method for n-butanol gas. Journal of Physics and Chemistry of Solids, 2018, 112, 43-49.	4.0	47
69	CeO2 nanoparticles modified by CuO nanoparticles for low-temperature CO oxidation with high catalytic activity. Journal of Physics and Chemistry of Solids, 2020, 147, 109651.	4.0	47
70	Dual-emission ratiometric fluorescent detection of dinotefuran based on sulfur-doped carbon quantum dots and copper nanocluster hybrid. Sensors and Actuators B: Chemical, 2020, 321, 128534.	7.8	46
71	Catalytic activity for CO oxidation of Cu–CeO <sub>2</sub> composite nanoparticles synthesized by a hydrothermal method. Analytical Methods, 2015, 7, 3238-3245.	2.7	45
72	Optical and gas sensing properties of Al-doped ZnO transparent conducting films prepared by sol–gel method under different heat treatments. Ceramics International, 2014, 40, 9931-9939.	4.8	43

#	Article	IF	CITATIONS
73	Self-grown MnO 2 nanosheets on carbon fiber paper as high-performance supercapacitors electrodes. Electrochimica Acta, 2016, 217, 16-23.	5.2	43
74	Hydrothermal growth of ZnO nanorods on Zn substrates and their application in degradation of azo dyes under ambient conditions. CrystEngComm, 2014, 16, 7761-7770.	2.6	42
75	Hierarchically porous carbon derived from the activation of waste chestnut shells by potassium bicarbonate (KHCO <sub>3</sub> ) for highâ€performance supercapacitor electrode. International Journal of Energy Research, 2020, 44, 988-999.	4.5	42
76	Enhanced methanol sensing properties of SnO <sub>2</sub> microspheres in a composite with Pt nanoparticles. RSC Advances, 2016, 6, 83870-83879.	3.6	41
77	Water-soluble ZnO quantum dots modified by (3-aminopropyl)triethoxysilane: The promising fluorescent probe for the selective detection of Cu2+ ion in drinking water. Journal of Alloys and Compounds, 2020, 825, 153904.	5.5	40
78	Macro-/meso-porous NiCo2O4 synthesized by template-free solution combustion to enhance the performance of a nonenzymatic amperometric glucose sensor. Mikrochimica Acta, 2020, 187, 64.	5.0	39
79	Carbon spheres@MnO2 core-shell nanocomposites with enhanced dielectric properties for electromagnetic shielding. Scientific Reports, 2017, 7, 15841.	3.3	38
80	Structure and catalytic activity of 3D macro/mesoporous Co3O4 for CO oxidation prepared by a facile self-sustained decomposition of metal–organic complexes. Journal of Molecular Catalysis A, 2015, 398, 79-85.	4.8	37
81	Effect of calcination temperatures on the electrochemical performances of nickel oxide/reduction graphene oxide (NiO/RGO) composites synthesized by hydrothermal method. Journal of Physics and Chemistry of Solids, 2016, 98, 209-219.	4.0	37
82	Flash synthesis of Al-doping macro-/nanoporous ZnO from self-sustained decomposition of Zn-based complex for superior gas-sensing application to n-butanol. Sensors and Actuators B: Chemical, 2016, 237, 90-98.	7.8	36
83	A designed Mn2O3/MCM-41 nanoporous composite for methylene blue and rhodamine B removal with high efficiency. Ceramics International, 2014, 40, 8093-8101.	4.8	35
84	TiO2 nanoparticles functionalized by Pd nanoparticles for gas-sensing application with enhanced butane response performances. Scientific Reports, 2017, 7, 7692.	3.3	35
85	Novel Al-doped CdIn2O4 nanofibers based gas sensor for enhanced low-concentration n-butanol sensing. Sensors and Actuators B: Chemical, 2022, 351, 130946.	7.8	35
86	A one-step nonaqueous sol–gel route to mixed-phase TiO <sub>2</sub> with enhanced photocatalytic degradation of Rhodamine B under visible light. CrystEngComm, 2016, 18, 1964-1975.	2.6	33
87	Sensitive and selective n-butanol gas detection based on ZnO nanocrystalline synthesized by a low-temperature solvothermal method. Physica E: Low-Dimensional Systems and Nanostructures, 2018, 103, 143-150.	2.7	33
88	Synthesis, characterization and room temperature photoluminescence properties of Al doped ZnO nanorods. Physica E: Low-Dimensional Systems and Nanostructures, 2012, 44, 1399-1405.	2.7	32
89	One-step hydrothermal synthesis of thioglycolic acid capped CdS quantum dots as fluorescence determination of cobalt ion. Scientific Reports, 2018, 8, 8953.	3.3	32
90	The Fluorescent Quenching Mechanism of N and S Co-Doped Graphene Quantum Dots with Fe3+ and Hg2+ Ions and Their Application as a Novel Fluorescent Sensor. Nanomaterials, 2019, 9, 738.	4.1	32

#	Article	IF	CITATIONS
91	Mn3O4/activated carbon composites with enhanced electrochemical performances for electrochemical capacitors. Journal of Alloys and Compounds, 2017, 703, 163-173.	5.5	31
92	Enhanced formaldehyde sensing properties of SnO <sub>2</sub> nanorods coupled with Zn <sub>2</sub> SnO <sub>4</sub> . RSC Advances, 2015, 5, 42628-42636.	3.6	30
93	Mesoporous CuCo2O4 rods modified glassy carbon electrode as a novel non-enzymatic amperometric electrochemical sensors with high-sensitive ascorbic acid recognition. Journal of Alloys and Compounds, 2021, 852, 157045.	5.5	30
94	Butane detection: W-doped TiO <sub>2</sub> nanoparticles for a butane gas sensor with high sensitivity and fast response/recovery. RSC Advances, 2015, 5, 96539-96546.	3.6	26
95	Flash synthesis of macro-/nanoporous ZnCo 2 O 4 via self-sustained decomposition of metal–organic complexes. Materials Letters, 2014, 134, 138-141.	2.6	25
96	Combustion synthesized hierarchically porous WO3 for selective acetone sensing. Materials Chemistry and Physics, 2016, 184, 155-161.	4.0	25
97	Citric Acid Capped CdS Quantum Dots for Fluorescence Detection of Copper Ions (II) in Aqueous Solution. Nanomaterials, 2019, 9, 32.	4.1	25
98	Enhanced and tunable fluorescent quantum dots within a single crystal of protein. Nano Research, 2013, 6, 627-634.	10.4	24
99	Portably colorimetric paper sensor based on ZnS quantum dots for semi-quantitative detection of Co2+ through the measurement of grey level. Sensors and Actuators B: Chemical, 2018, 260, 1068-1075.	7.8	24
100	Grey level replaces fluorescent intensity: Fluorescent paper sensor based on ZnO nanoparticles for quantitative detection of Cu2+ without photoluminescence spectrometer. Sensors and Actuators B: Chemical, 2018, 255, 2356-2366.	7.8	24
101	Preparation and photoluminescence properties of organic–inorganic nanocomposite with a mesolamellar nickel oxide. Microporous and Mesoporous Materials, 2004, 71, 99-102.	4.4	23
102	A facial method to synthesize Ni(OH)2 nanosheets for improving the adsorption properties of Congo red in aqueous solution. Powder Technology, 2013, 235, 121-125.	4.2	23
103	The electrochemical performances of NiCo2O4 nanoparticles synthesized by one-step solvothermal method. Ionics, 2017, 23, 2457-2463.	2.4	23
104	Synthesis of mixed Mn–Ce–Ox one dimensional nanostructures and their catalytic activity for CO oxidation. Ceramics International, 2015, 41, 4675-4682.	4.8	22
105	A nonaqueous sol–gel route to synthesize CdIn2O4 nanoparticles for the improvement of formaldehyde-sensing performance. Scripta Materialia, 2009, 61, 935-938.	5.2	21
106	A low temperature butane gas sensor used Pt nanoparticles-modified AZO macro/mesoporous nanosheets as sensing material. Sensors and Actuators B: Chemical, 2018, 254, 227-238.	7.8	21
107	Nonaqueous synthesis of Pd-functionalized SnO2/In2O3 nanocomposites for excellent butane sensing properties. Sensors and Actuators B: Chemical, 2018, 257, 419-426.	7.8	21
108	Ag-Functionalized macro-/mesoporous AZO synthesized by solution combustion for VOCs gas sensing application. RSC Advances, 2016, 6, 101304-101312.	3.6	20

#	Article	IF	CITATIONS
109	Rhodamine B assisted graphene quantum dots flourescent sensor system for sensitive recognition of mercury ions. Journal of Luminescence, 2019, 207, 273-281.	3.1	20
110	One-dimensional In <sub>2</sub> O <sub>3</sub> nanorods as sensing material for ppb-level n-butanol detection. Nanotechnology, 2021, 32, 375501.	2.6	20
111	RGO/KMn8O16 composite as supercapacitor electrode with high specific capacitance. Ceramics International, 2016, 42, 5195-5202.	4.8	19
112	Synthesis of core-shell carbon sphere@nickel oxide composites and their application for supercapacitors. Ionics, 2018, 24, 513-521.	2.4	19
113	Nanosheets based mixed structure CuCo2O4 hydrothermally grown on Ni foam applied as binder-free supercapacitor electrodes. Journal of Energy Storage, 2020, 32, 101865.	8.1	19
114	Oxygen vacancies promoted heterogeneous catalytic ozonation of atrazine by defective 4A zeolite. Journal of Cleaner Production, 2022, 336, 130376.	9.3	18
115	DNAâ€Encoded Tuning of Geometric and Plasmonic Properties of Nanoparticles Growing from Gold Nanorod Seeds. Angewandte Chemie, 2015, 127, 8232-8236.	2.0	17
116	Enhancing phosphate removal from water by using ordered mesoporous silica loaded with samarium oxide. Analytical Methods, 2015, 7, 10052-10060.	2.7	17
117	Synthesis, characterization and photoluminescent properties of rare-earth hydroxides and oxides nanorods by hydrothermal route. Applied Physics A: Materials Science and Processing, 2013, 111, 1229-1240.	2.3	16
118	A novel microwave absorption material of Ni doped cryptomelane type manganese oxides. Ceramics International, 2015, 41, 5688-5695.	4.8	16
119	CdIn2O4 nanoporous thin film gas-sensor for formaldehyde detection. Physica E: Low-Dimensional Systems and Nanostructures, 2018, 103, 18-24.	2.7	16
120	Excellent fluorescence detection of Cu <sup>2+</sup> in water system using N-acetyl-L-cysteines modified CdS quantum dots as fluorescence probe. Nanotechnology, 2021, 32, 405707.	2.6	16
121	Partially oxidized Ti3C2Tx MXene-sensitive material-based ammonia gas sensor with high-sensing performances for room temperature application. Journal of Materials Science: Materials in Electronics, 2021, 32, 27837-27848.	2.2	16
122	Binder-free three-dimensional interconnected CuV <sub>2</sub> O <sub>5</sub> · <i>n</i> H <sub>2</sub> O nests as cathodes for high-loading aqueous zinc-ion batteries. Inorganic Chemistry Frontiers, 2022, 9, 792-804.	6.0	16
123	Trimetallic metal-organic frameworks (Fe, Co, Ni-MOF) derived as efficient electrochemical determination for ultra-micro imidacloprid in vegetables. Nanotechnology, 2022, 33, 135502.	2.6	16
124	One-pot synthesis of N-doped graphene quantum dots as highly sensitive fluorescent sensor for detection of mercury ions water solutions. Materials Research Express, 2019, 6, 095615.	1.6	15
125	Pt decorated SnO2 nanoparticles for high response CO gas sensor under the low operating temperature. Journal of Materials Science: Materials in Electronics, 2019, 30, 3921-3932.	2.2	15
126	Pd-Functionalized SnO2 Nanofibers Prepared by Shaddock Peels as Bio-Templates for High Gas Sensing Performance toward Butane. Nanomaterials, 2019, 9, 13.	4.1	15

#	Article	IF	CITATIONS
127	Amino-capped zinc oxide modified tin oxide electron transport layer for efficient perovskite solar cells. Cell Reports Physical Science, 2021, 2, 100590.	5.6	15
128	NiO nanosheets assembled into hollow microspheres for highly sensitive and fast-responding VOC sensors. RSC Advances, 2015, 5, 80786-80792.	3.6	14
129	Macro-/nanoporous Al-doped ZnO via self-sustained decomposition of metal-organic complexes for application in degradation of Congo red. Ceramics International, 2016, 42, 18914-18924.	4.8	14
130	Facile synthesis of CuO micro-sheets over Cu foil in oxalic acid solution and their sensing properties towards n-butanol. Journal of Materials Chemistry C, 2016, 4, 985-990.	5.5	14
131	Ptâ€Functionalized Nanoporous TiO <sub>2</sub> Nanoparticles With Enhanced Gas Sensing Performances Toward Acetone. Physica Status Solidi (A) Applications and Materials Science, 2018, 215, 1800100.	1.8	14
132	Fluorescent ZnO quantum dots synthesized with urea for the selective detection of Cr <sup>6+</sup> ion in water with a wide range of concentrations. Methods and Applications in Fluorescence, 2019, 7, 035007.	2.3	14
133	Synthesis and characterization of ordered hexagonal and cubic mesoporous tin oxides via mixed-surfactant templates route. Journal of Colloid and Interface Science, 2005, 286, 627-631.	9.4	13
134	Facile synthesis and gas sensing performances based on nickel oxide nanoparticles/multi-wall carbon nanotube composite. Journal of Materials Science: Materials in Electronics, 2015, 26, 8240-8248.	2.2	13
135	Nanoporous network SnO2 constructed with ultra-small nanoparticles for methane gas sensor. Journal of Materials Science: Materials in Electronics, 2019, 30, 14325-14334.	2.2	13
136	Sm-doped SnO2 nanoparticles synthesized via solvothermal method as a high-performance formaldehyde sensing material for gas sensors. Journal of Materials Science: Materials in Electronics, 2021, 32, 8249-8264.	2.2	13
137	From Water and Ni Foam to a Ni(OH) <sub>2</sub> @Ni Foam Binderâ€Free Supercapacitor Electrode: A Green Corrosion Route. ChemElectroChem, 2018, 5, 434-444.	3.4	12
138	Flash Synthesis and CO Oxidation of Macro-/Nano-porous Co3O4–CeO2 Via Self-Sustained Decomposition of Metal–Organic Complexes. Catalysis Letters, 2015, 145, 1344-1350.	2.6	11
139	Ag decorated ZnO nanocrystallines synthesized by a low-temperature solvothermal method and their application for high response H2 gas sensor. Journal of Materials Science: Materials in Electronics, 2019, 30, 18959-18969.	2.2	11
140	Electrochemical zinc and hydrogen co-intercalation in Li3(V6O16): A high-capacity aqueous zinc-ion battery cathode. Electrochimica Acta, 2022, 412, 140120.	5.2	11
141	Porous cobaltate: Structure, active sites, thermocatalytic properties for ammonium perchlorate decomposition. Journal of Alloys and Compounds, 2022, 908, 164624.	5.5	11
142	Synthesis, characterization and room temperature photoluminescence properties of briers-like ZnO nanoarchitectures. Materials Science and Engineering B: Solid-State Materials for Advanced Technology, 2010, 167, 177-181.	3.5	10
143	L-Aspartic Acid Capped CdS Quantum Dots as a High Performance Fluorescence Assay for Sliver Ions (I) Detection. Nanomaterials, 2019, 9, 1165.	4.1	10
144	Hierarchitecture Co 2 (OH) 3 Cl@FeCo 2 O 4 composite as a novel and highâ€performance electrode material applied in supercapacitor. International Journal of Energy Research, 2020, 44, 3122-3133.	4.5	10

#	Article	IF	CITATIONS
145	Multi-sized nanosheets cobalt-iron layered double hydroxide grown on nickel foam as high performance supercapacitor electrode material. Journal of Energy Storage, 2021, 33, 102088.	8.1	10
146	Formation of manganite fibers under the directing of cationic surfactant. Materials Science and Engineering C, 2006, 26, 653-656.	7.3	9
147	Structure, morphologies and dye removal efficiency of ZnO nanorods grown on polycrystalline Zn substrate. Superlattices and Microstructures, 2014, 74, 279-293.	3.1	9
148	Surfactant-mediated synthesis of ZnCo2O4 powders as a high-performance anode material for Li-ion batteries. Ionics, 2015, 21, 623-628.	2.4	9
149	Thioglycolic acid-capped ZnSe quantum dots as nanoprobe for cobalt(II) and iron(III) via measurement of grey level, UV-vis spectra and dynamic light scattering. Mikrochimica Acta, 2019, 186, 444.	5.0	9
150	Nickel foam electrode decorated with Fe-CdIn2O4 nanoparticles as an effective electrochemical sensor for non-enzymatic glucose detection. Journal of Electroanalytical Chemistry, 2022, 919, 116524.	3.8	9
151	β-MnO2 microrods for the degradation of methyl orange under acid condition from aqueous solutions. Research on Chemical Intermediates, 2017, 43, 3975-3987.	2.7	8
152	Combustion agent mediated flash synthesis of porous MCo 2 O 4 (M = Zn, Ni, Cu and Fe) via self-sustained decomposition of metal-organic complexes. Materials Letters, 2017, 195, 123-126.	2.6	8
153	â€~Green' prepare SnO2 nanofibers by shaddock peels: application for detection of volatile organic compound gases. Journal of Materials Science: Materials in Electronics, 2019, 30, 3032-3044.	2.2	8
154	Novel method for the qualitative identification of chromium ions (III) using l-aspartic acid stabilized CdS quantum dots. Journal of Physics and Chemistry of Solids, 2020, 136, 109160.	4.0	8
155	Potassium sulphate (K 2 SO 4 ) activation of chestnut shell to oxygenâ€enriched porous carbons with enhanced capacitive properties. International Journal of Energy Research, 2020, 44, 5385-5396.	4.5	8
156	FACILE SYNTHESIS AND MICROWAVE ABSORPTION PROPERTIES OF $\hat{1}$ ±-MnO2 NANORODS. Functional Materials Letters, 2012, 05, 1250043.	1.2	7
157	A novel non-enzymatic glucose electrochemical sensor with high sensitivity and selectivity based on CdIn <sub>2</sub> O <sub>4</sub> nanoparticles on 3D Ni foam substrate. Nanotechnology, 2021, 32, 405502.	2.6	7
158	Preparation of NaV <sub>6</sub> O <sub>15</sub> Nanosheet Cathodes with High Cycling Performance and Good Capacity Retention Rate in Aqueous Zincâ€ion Batteries. Physica Status Solidi (A) Applications and Materials Science, 2022, 219, .	1.8	7
159	Combustion synthesized hierarchically porous Mn <sub>3</sub> O <sub>4</sub> for catalytic degradation of methyl orange. Canadian Journal of Chemical Engineering, 2017, 95, 643-647.	1.7	6
160	From Water and Ni Foam to a Ni(OH)2 @Ni Foam Binder-Free Supercapacitor Electrode: A Green Corrosion Route. ChemElectroChem, 2018, 5, 409-409.	3.4	4
161	SnO2 quantum dots with rapid butane detection at lower ppm-level. Applied Physics A: Materials Science and Processing, 2018, 124, 1.	2.3	4
162	High-performance non-enzymatic glucose sensors based on porous Co3O4 synthesized by coprecipitation method with the different precipitants. Ionics, 2021, 27, 1803-1812.	2.4	4

#	Article	IF	CITATIONS
163	ZnO-SnO2 nanocomposites modified by PdO nanoparticles named PdO-ZSO as gas sensing material for hydrogen and butane with the excellent response time and recovery time. Journal of Materials Science: Materials in Electronics, 2021, 32, 28891-28908.	2.2	4
164	Gas response enhancement of VOCs sensor based on Sn doped nanoporous anatase TiO <sub>2</sub> nanoparticles at a relative low operating temperature. Materials Research Express, 2019, 6, 105008.	1.6	3
165	Fluorescence â€~turn-on' probe for Al <sup>3+</sup> Âdetection in water based on ZnS/ZnO quantum dots with excellent selectivity and stability. Nanotechnology, 2021, 32, 375001.	2.6	2
166	V <sub>2</sub> O <sub>5</sub> /NaV <sub>6</sub> O <sub>15</sub> nanocomposites synthesized by molten salt method as a high-performances cathode material for aqueous zinc-ion batteries. Nanotechnology, 2022, 33, 115402.	2.6	2
167	Preparation, characterization and room temperature photoluminescence properties of a zinc oxide nanosheet network grown on glass substrate by a facile chemical route. Superlattices and Microstructures, 2011, 50, 311-318.	3.1	1
168	Electrocatalytic performance of mesoporous NiCo2O4 nanosheets with elemental electron synergy towards direct glucose in alkaline solution. Journal of Physics and Chemistry of Solids, 2022, 167, 110784.	4.0	0